Algorithm for preliminary analysis of diffraction patterns of nanocomposite materials with an admixture of a bulk component

© *O.A. Alekseeva,*[1,2] *A.A. Naberezhnov*[3]

[1] Peter the Great Saint-Petersburg Polytechnic University,
St. Petersburg, Russia
[2] Tomsk State University of Control Systems and Radioelectronics,
Tomsk, Russia
[3] Ioffe Institute,
St. Petersburg, Russia
e-mail: alex.nabereznov@mail.ioffe.ru

This contribution is devoted to discussion of questions related to the influence of a possible contribution from a bulk material on the lineshape of elastic peaks observed in diffraction experiments at neutron and/or X-ray radiation scattering on nanoporous matrices containing substances embedded into their porous space (channels). The proposed algorithm permits to estimate the input of massive component into diffraction peaks using the analysis of the experimentally observed distortions of the lineshape of Bragg peaks. This preliminary analysis greatly simplifies the profile analysis of nanocomposite diffraction patterns, especially for molecular sieves based on powders of SBA-15, MCM-41, MCM-48, etc. types.

Keywords: porous matrices, diffraction, nanocomposite materials, elastic peak lineshape, higher central distribution moments

Introduction

Diffraction methods rank among the essential techniques for research into nanocomposite materials (NCMs), since the analysis of diffraction spectra provides a considerable amount of useful data on the NCM structure (and its temperature evolution), the specifics of phase transitions in these materials, the internal arrangement of nanoparticles in pores of the initial matrices (including their sizes and shape anisotropy), etc. However, difficulties arise in certain cases in the final processing of experimental data, since NCMs (especially those produced based on molecular sieves type SBA-15, MCM-41, MCM-48, etc.) may contain an admixture of a bulk material that distorts considerably the general picture of the observed phenomena. For example, it was demonstrated in [1] that the experimentally observed temperature hysteresis in the behavior of the order parameter in NCMs produced based on powders of porous molecular sieves 2D-SBA-15 and 3D-SBA-15, which contain ferroelectric $NaNO_2$ in pores, is induced not only by size effects and properties of the matrix itself, but also by the presence of admixed bulk sodium nitrate. According to the refined data obtained by differential scanning calorimetry and after the application of the procedure detailed in the present study, bulk sodium nitrate constitutes about 20% of the overall $NaNO_2$ content of the sample. If admixed bulk material is present in an NCM, a full-scale diffraction experiment and full-profile analysis of the obtained diffraction patterns are often needed. This is not always possible (especially at the stage of production of an NCM). The proposed algorithm allows one to determine the bulk fraction rather quickly and with only a single intense peak available for analysis. Thus, it becomes possible to perform preliminary testing of an NCM, estimate the quality of the prepared sample, and schedule the time needed for full-scale examination of the structure (and its temperature evolution) of the given NCM (i.e., estimate the time required to accumulate a sufficient data set with the contribution of a bulk material taken into account).

1. Calculation procedure

1.1. Initial parameters and conditions

The availability of data on the instrumental resolution of the measurement instrument (above all, the dependence of the elastic peak width on angle θ of scattering of incident radiation or on the interplanar distance) is one of the key initial conditions. These data and information regarding the parameters of the function characterizing the lineshape of the elastic peak are necessarily provided in the datasheet of the experimental setup and are available in advance. As a rule, they are verified with the use of reference samples at least once in six months. In the present study, we used the setup parameters of FIREPOD E9 (Helmholtz Zentrum Berlin, Germany) high-resolution neutron diffractometer as an example. Instrumental broadening H_{inst} of the elastic

peak was calculated as

$$H_{instr}^2 = U \operatorname{tg}^2 \theta + V \operatorname{tg} \theta + W, \qquad (1)$$

where parameters U, V, W were taken from the datasheet.

It was assumed that the width of the reflection line corresponding to the bulk phase was defined solely by the instrumental resolution and the broadening (both for the bulk material and the NCM) due to possible elastic stress was absent.

The width of the line of the elastic peak corresponding to the nanostructured phase was calculated as the sum of contributions from instrumental and size broadenings.

In general, the width of elastic reflections in an NCM may increase for two reasons: due to the size effect (broadening is then proportional to $\sim 1/\cos\theta$) and due to the internal stress in nanoparticles (broadening is then proportional to $\tan\theta$). In the general case, the Williamson–Hall formula is used [2–4]:

$$B \cos\theta = \eta \sin\theta + k\lambda/d, \qquad (2)$$

where λ is the radiation wavelength in angstroms, B is the peak broadening (FWHM) determined with the function characterizing the shape of the maximum and the resolution function taken into account (see example in [3,4]), d is the diffraction particle size, η is the internal stress, 2θ is the Bragg peak position, and k is the shape parameter, which is usually $\sim 0.9-1$. It was assumed in our calculations that $k = 1$. It is seen clearly from the above that the contributions have different dependences on the scattering angle and may be distinguished easily. Therefore, below we limit ourselves to a rather small scattering angle at which the contribution from internal stress to broadening may be neglected. The Debye–Scherrer approach is then applicable:

$$H_{size} = \frac{k\lambda}{d\cos\theta}. \qquad (3)$$

The evolution of shape of the (100) peak of the cubic structure with unit cell parameter $a = 3.35\,\text{Å}$ was examined in simulation of the response. The wavelength of incident neutrons was $\lambda = 1.7982(1)\,\text{Å}$. Two values of parameter a were used in calculations for the nanostructured material in pores: $3.35\,\text{Å}$ (as for the bulk) and $3.345\,\text{Å}$.

1.2. Calculation details

Three different functions characterizing both the instrumental resolution and the lineshape of an experimental elastic peak were considered: Gaussian, Lorentzian, and Voigt functions. Mixed cases (i.e., when the instrumental function is Gaussian and the experimental spectrum is characterized using the Lorentzian function) were not considered. The evolution of shape (and parameters characterizing it) of the elastic peak was then calculated as function of the weight percentage of the bulk material, the diffraction size of nanoparticles, and the above-mentioned difference in unit cell parameters.

The contributions due to instrumental broadening and size broadening were summed in accordance with the following formulae:

for a Gaussian line profile, FWHM H_G was determined as

$$H_G^2 = H_{instr}^2 + H_{size}^2, \qquad (4)$$

for a Lorentzian profile,

$$H_L = H_{instr} + H_{size}, \qquad (5)$$

for a line profile characterized by the Voigt function, which is, by definition, a convolution of a Lorentzian and a Gaussian:

$$V(x) = L(x) \otimes G(x) = \int\limits_{-\infty}^{+\infty} L(x-u)G(u)\,du \qquad (6)$$

(here, $L(x)$ and $G(x)$ are the components characterized by a Lorentzian and a Gaussian, respectively, with different FWHM values H_L and H_G), numerical approximation of expression (6) in the form of a linear combination of Lorentzian $L'(x)$ and Gaussian $G'(x)$ contributions (the so-called pseudo-Voigt function) with the same FWHM H_{pV} was used:

$$pV(x) = \eta L'(x) + (1-\eta)G'(x), \qquad (7)$$

parameters η and H_{pV} of pseudo-Voigt function $pV(x)$ were expressed in terms of H_G and H_L, which are defined by (4) and (5), and calculated in accordance with the approach proposed in [5]:

$$H_{pV}^5 = H_G^5 + 2.69269H_G^4 H_L + 2.42843 H_G^3 H_L^2$$
$$+ 4.47163 H_G^2 H_L^3 + 0.07842 H_G H_L^4 + H_L^5, \qquad (8)$$

$$\eta = 1.36603\frac{H_L}{H_{pV}} - 0.47719\left(\frac{H_L}{H_{pV}}\right)^2 + 0.11116\left(\frac{H_L}{H_{pV}}\right)^3. \qquad (9)$$

At the next stage, the behavior of dispersion σ, asymmetry coefficient γ_1, and coefficient of excess γ_2, was analyzed. They were expressed in terms of the second, the third, and the fourth moments about mean μ_2, μ_3, μ_4 for simulated distributions of intensity of elastic peaks and calculated using the following formulae [6]:

$$\sigma = \sqrt{\mu_2}, \;\; \gamma_1 = \frac{\mu_3}{\sigma^3}, \;\; \gamma_2 = \frac{\mu_4}{\sigma^4} - 3,$$

to calculate the moments for line profiles characterized by Lorentzian and Voigt functions, integration was performed over a finite interval symmetric with respect to the peak maximum, since the integrals defining higher-order moments for these functions are undefined on an infinite interval. The calculations results are presented in Figs. 1−4.
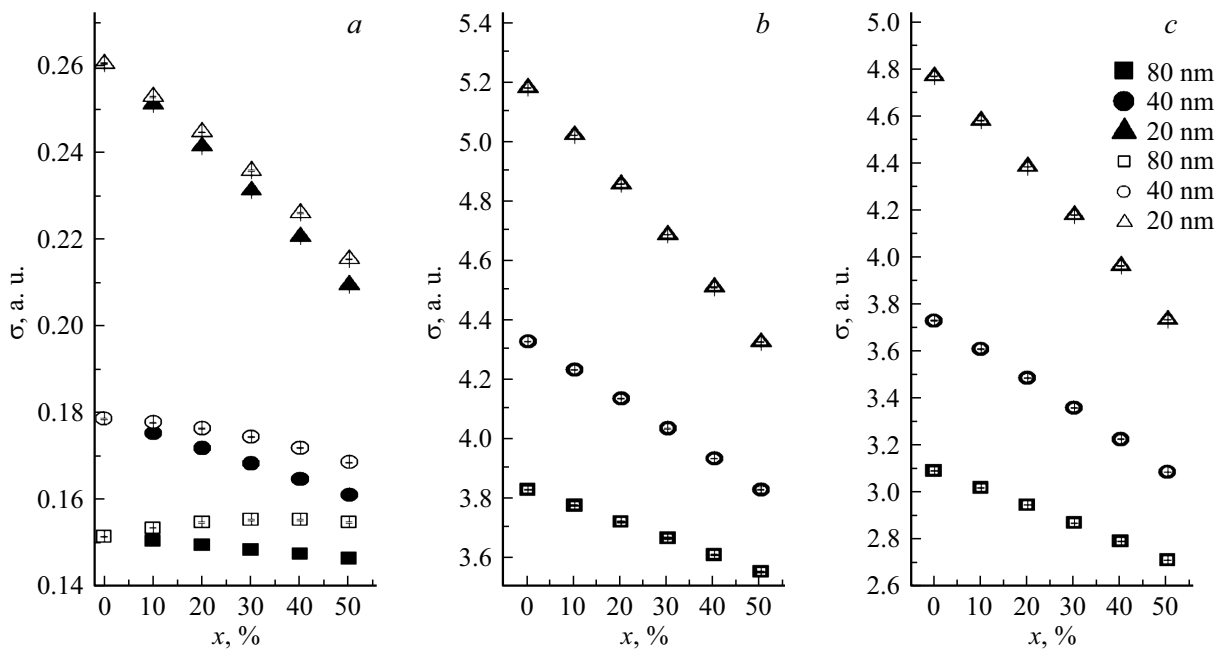
Figure 1. Variation of dispersion (σ) of the lineshape of Bragg reflection with an increase in the weight percentage of the bulk phase in the sample (x) for different line profile functions (Gaussian (a), Lorentzian (b), and pseudo-Voigt (c)), particle sizes, and ratios of lattice parameters of the bulk and nanostructured phases (filled symbols: lattice parameters are equal; open symbols: lattice parameters of the bulk and nanostructured phases differ).
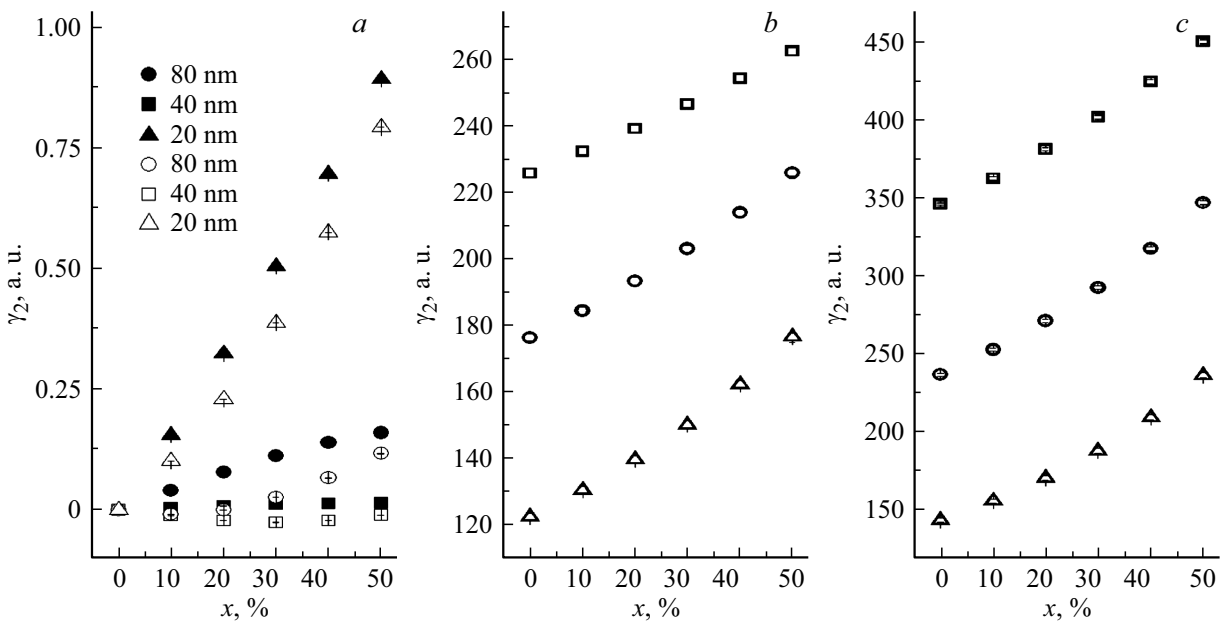
Figure 2. Variation of the coefficient of excess (γ_2) of Bragg reflection with an increase in the weight percentage of the bulk phase in the sample (x) for different line profile functions (Gaussian (a), Lorentzian (b), and pseudo-Voigt (c)), particle sizes, and ratios of lattice parameters of the bulk and nanostructured phases (filled symbols: lattice parameters are equal; open symbols: lattice parameters of the bulk and nanostructured phases differ).

2. Results and discussion

Figure 1 presents the results of calculation of the dependence of parameter σ on the admixture of a bulk material at different nanoparticle sizes (indicated in the figure) for

Gaussian (Fig. 1, a), Lorentzian (Fig. 1, b), and pseudo-Voigt (Fig. 1, c) functions. Note that filled symbols in all figures correspond to the case when the unit cell parameters for the bulk fraction and the nanostructured material are the same. The estimated error of calculations is also shown and
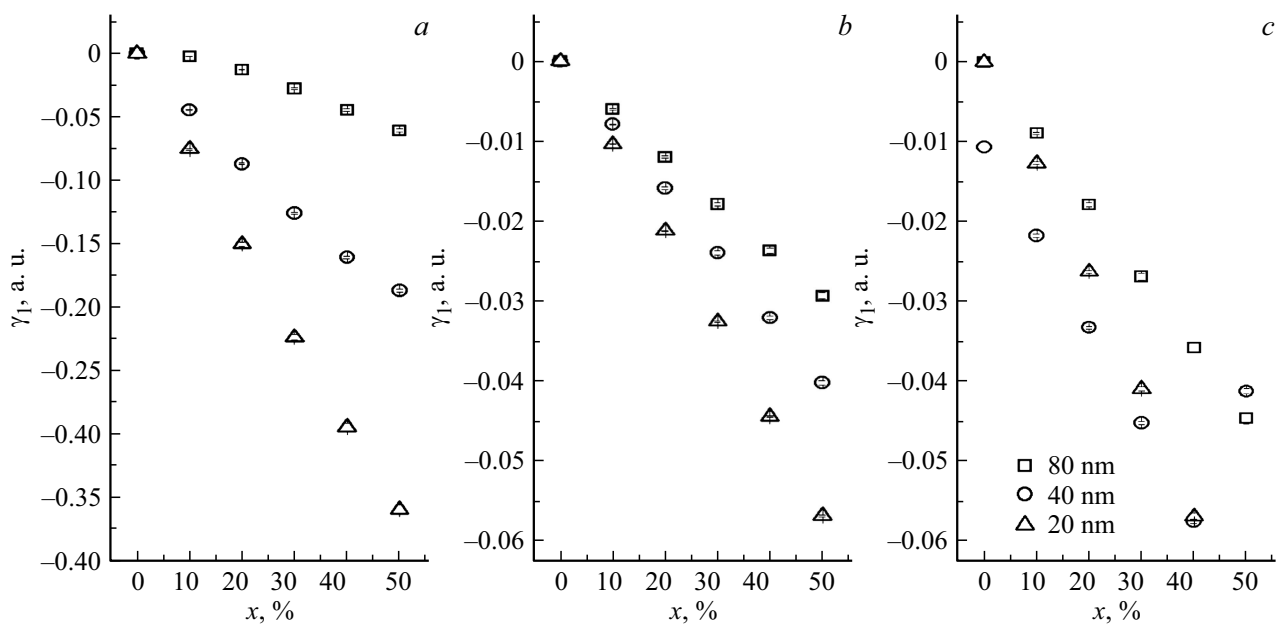
Figure 3. Variation of the asymmetry coefficient (γ_1) of Bragg reflection with an increase in the weight percentage of the bulk phase in the sample (x) for different line profile functions (Gaussian (a), Lorentzian (b), and pseudo-Voigt (c)) and particle sizes.

usually does not exceed the size of a symbol. The lineshape dispersion decreases as the weight percentage of the bulk material increases. This variation becomes more apparent as particles become smaller in size. The dependence on the difference between lattice parameters a is also well-pronounced. If two Lorentzians (Fig. 1, b) or two pseudo-Voigt functions (Fig. 1, c) are used to characterize the instrumental resolution and the experimental elastic peak, the cases of different and equal lattice parameters become indistinguishable within the error limits (filled and open symbols coincide), and only the dependence of σ on the bulk phase admixture remains. Note that the positions of the maxima of distributions naturally depend on the difference between unit cell parameters. It can be seen from Fig. 1 that a fairly reliable estimate of the percentage contribution of the bulk phase may be obtained by analyzing the dispersion data only: this contribution is no lower than 10% for Gaussian and Lorentzian functions (for nanoparticles with a characteristic size below 80 nm) and approximately 5% for the pseudo-Voigt function (for all the studied nanoparticle sizes).

Let us now examine the dependence of the coefficient of excess (γ_2) on the bulk phase percentage (Fig. 2). Figure 2 demonstrates clearly that this coefficient increases with the bulk fraction percentage regardless of the type of the profile function, the size of particles, and the ratio of lattice parameters. The most pronounced growth of γ_2 corresponds to the smallest particles for all three profiles. Again, a fairly reliable estimate of the percentage contribution of the bulk phase may be obtained: this contribution is no lower than 10% for the Gaussian function (for nanoparticles with a characteristic size below 80 nm) and approximately 5% for Lorentzian and pseudo-Voigt

functions (for all the studied nanoparticle sizes). In addition, just as in Fig. 1, parameter γ_2 is almost independent of the difference between the unit cell parameters for Lorentzian (Fig. 2, b) and pseudo-Voigt functions (Fig. 2, c): filled and open symbols coincide.

Next, we examine the behavior of asymmetry coefficient γ_1. It is evident that the corresponding lineshape distortions are related in this case to the difference between lattice parameters a for bulk and nanostructured materials. Therefore, the results of calculations only for the case of differing parameters and for all the functions mentioned earlier are presented in Fig. 3. It should be noted immediately that the magnitude of coefficient γ_1 increases with the weight percentage of the bulk phase; i.e., the larger the particles, the greater the γ_1 coefficient. It is seen clearly that this variation (i.e., the difference between the values of γ_1 at different weight percentages of the bulk phase and different diffraction sizes of nanoparticles) for the Gaussian function (Fig. 3, a) is significantly stronger than the corresponding variation for the Lorentzian and pseudo-Voigt profiles.

It follows from Fig. 3, a that the lineshape asymmetry of the elastic peak may well be measured experimentally for an NCM containing, alongside with nanoparticles with a characteristic size of 40 and 20 nm, at least 5% of a bulk material. As for larger nanoparticles (80 nm), 5% admixture of the bulk phase also becomes detectable for the Lorentzian and pseudo-Voigt functions (Figs. 3, b and 3, c).

At the last stage, we have used formulae (4), (5), (7), and (9) to calculate the dependences of the FWHM values (in degrees) for all the cases examined above (Fig. 4) for the FIREPOD E9 high-resolution neutron diffractometer.
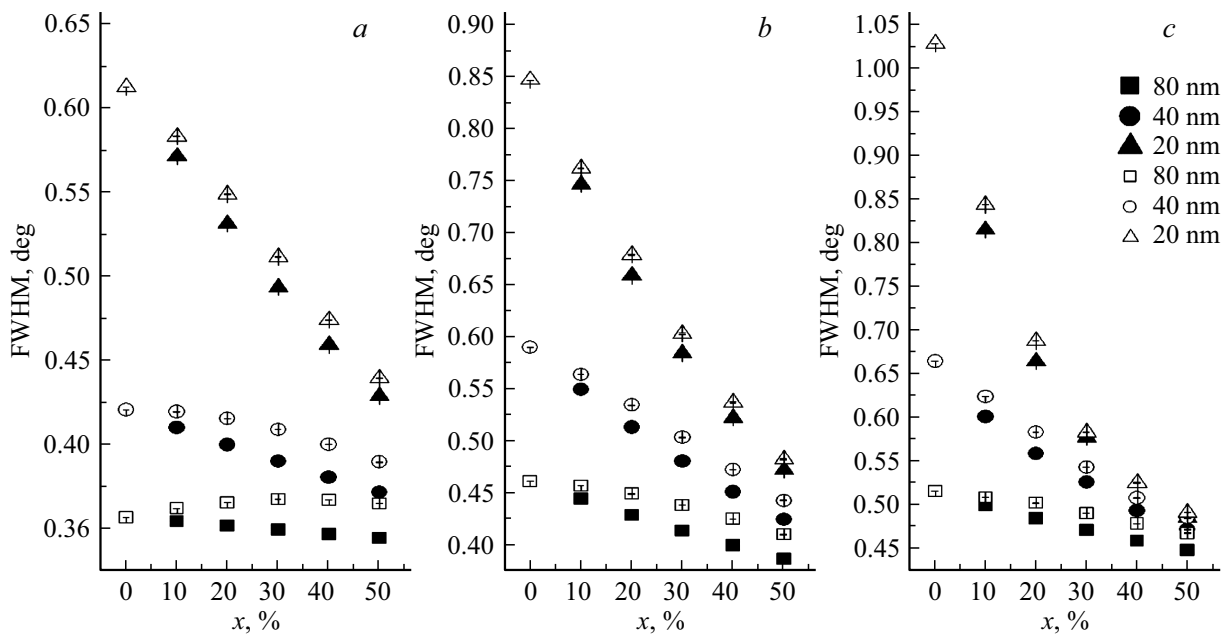
Figure 4. Variation of the full width at half maximum (FWHM) of Bragg reflection with an increase in the weight percentage of the bulk phase in the sample (x) for different line profile functions (Gaussian (a), Lorentzian (b), and pseudo-Voigt (c)), particle sizes, and ratios of lattice parameters of the bulk and nanostructured phases (filled symbols: lattice parameters are equal; open symbols: lattice parameters of the bulk and nanostructured phases differ).

The dependences in Fig. 4 demonstrate clearly that a fairly reliable estimate of the bulk material admixture at a level of 5% for small nanoparticles (with a diffraction size below 80 nm) may be obtained just by analyzing the FWHM values. In fact, one may even estimate the difference in unit cell parameters (if such a difference exists). Thus, the following algorithm for preliminary testing (by neutron or X-ray diffraction) of nanocomposite materials with a possible admixture of a bulk material may be formulated based on the above considerations:

1. A model spectrum is calculated with the instrumental resolution taken into account and for several possible (expected) diffraction sizes of nanoparticles introduced into the pores of the matrix used. Futher FWHM values and moments σ, γ_1, γ_2 are calculated.

2. Fine-resolution measurements of a single (in the case of a cubic structure) intense reflection are performed at small scattering angles for the empty matrix and the bulk material in the region of the chosen peak. The FWHM values and moments σ, γ_1, γ_2 of the obtained angular distribution of intensity for the bulk phase and the NCM with the empty-matrix background subtracted are then analyzed. At the same time, it is necessary to ensure enough statistics to make the observed broadening has been beyond the errors of FWHM determination.

3. The results of comparison of parameters of simulated and experimental spectra are used to estimate the size of a nanoparticle, its lattice parameters, and the bulk material content (in certain cases, with an accuracy up to 5 percent by weight; see above).

In our view, the proposed procedure may prove to be useful in production of NCMs based on molecular sieves, since it does not involve full-scale diffraction measurements and full-profile analysis of the obtained data, is not time-consuming, and is applicable even at low-resolution diffrac-tometers (only an accurately determined resolution function of the setup and extensive statistics are needed) in the case of nanoparticles with a small diffraction size. The procedure may also be used to evaluate the parameters of NCMs based on other porous matrices where the formation of large agglomerates in cracks, voids, and other similar matrix defects is possible.

Conclusion

A method allowing one to obtain data on the probable weight percentage of a bulk material in a nanocomposite material and estimate the size and parameters of the crystal structure of nanoparticles in this NCM by analyzing the parameters of a single diffraction peak for NCMs based on nanoporous matrices has been discussed. In future studies, we plan to examine the case of mixed functions characterizing the instrumental resolution and the NCM diffraction peak (e.g., Gaussian and Lorentzian or Gaussian and pseudo-Voigt functions) and the case when an NCM contains, apart from bulk and nanostructured materials, an amorphous phase.

Funding

Conflict of interest

The authors declare that they have no conflict of interest.

References

[1] A.A. Naberezhnov, E.V. Stukova, O.A. Alekseeva, S.A. Novikova, A. Franz. Tech. Phys., **64** (12), 1866 (2019). DOI: 10.1134/S106378421912020X

[2] G.K. Williamson, W.H. Hall. Acta Metallurgica, **1**, 22 (1953). DOI: 10.1016/0001-6160(53)90006-6

[3] V.D. Mote, Y. Purushotham, B.N. Dole. J. Theor. Appl. Phys., **6**, 6 (2012). DOI: 10.1186/2251-7235-6-6

[4] Y.T. Prabhu, K.V. Rao, V.S.S. Kumar, B.S. Kumari. World J. Nano Sci. Eng., **4**, 21 (2014). DOI: 10.4236/wjnse.2014.41004

[5] P. Thompson, D.E. Cox, J.B. Hastings. J. Appl. Cryst., **20**, 79 (1987). DOI: 10.1107/S0021889887087090

[6] H. Cramer, *Mathematical Methods of Statistics* (Princeton Univ. Press, 1946).